Symbol Detection of Ambient Backscatter Communications under IQ Imbalance

Yinghui Ye, Jiajia Zhao, Xiaoli Chu, *Senior Member, IEEE*, Sumei Sun, *Fellow, IEEE*, and Guangyue Lu

***Abstract*—Ambient backscatter communications (AmBC) have been mainly studied under the assumption of perfect inphase/quadrature-phase (IQ) balance, which is hard to achieve in practical AmBC networks. In this paper, we study the symbol detection in AmBC under IQ imbalances. In particular, considering a differential encoding scheme at the AmBC transmitter and an energy difference based detector at the AmBC receiver, we derive the bit error rate (BER) and the near-optimal detection threshold in closed forms. Since the near-optimal detection threshold requires a priori knowledge of the channel state information, the IQ imbalance parameters, the noise power and the transmit power of the ambient source, which is not readily known by the AmBC receiver, we propose a simple but practical method to estimate the near-optimal detection threshold by exploiting the received signal samples at the AmBC receiver. Simulation results validate the accuracy of the derived BER and detection threshold, and reveal that the studied detector is more robust to the amplitude imbalance than to the phase imbalance.**

***Index Terms*—Ambient backscatter communications, IQ imbalance, symbol detection.**

I. Introduction

Ambient backscatter communications (AmBC) have been deemed a strong contender for low-power and low-cost Internet of Things (IoT) [1], [2], where an IoT node acts as an AmBC transmitter to modulate and backscatter incident ambient signals, e.g., cellular signals, to realize information transmission, and the AmBC receiver receives the ambient source signal and the backscattered signal simultaneously. Since the ambient source signal is usually much stronger than the backscattered signal but is unknown by the AmBC receiver, it is not a trivial task to detect the AmBC information symbols from the composite received signal.

Leveraging the fact that the modulation rate of the ambient source signal is much higher than that of the AmBC signal, the authors in [3] eliminated the ambient source signal by averaging the composite received signal over multiple ambient source information symbols. Following this idea, a coherent-based energy detector with an optimal detection threshold to minimize bit error rate (BER) was proposed in [4], which however required the channel state information (CSI). To cope with this issue, by introducing the differential encoding into AmBC, a non-coherent energy-based detector and an energy difference based detector were designed in [5] and [6], respectively, and the corresponding near-optimal detection thresholds were derived. Subsequently, the non-coherent energy-based detector was extended from binary modulation to high-order modulation for the AmBC transmitter [7]. For multi-antenna AmBC receivers, a maximum-eigenvalue-based detector [8] and a generalized likelihood ratio test based detector [9] were proposed. In [10], the authors introduced orthogonal frequency division multiplexing into AmBC, and jointly designed the OFDM waveform and symbol detector for AmBC to cancel out the ambient source signal. The application of deep learning in AmBC to improve the symbol detection performance was studied in [11].

All these studies on symbol detectors in AmBC have largely ignored the hardware impairments (HIs), such as inphase/quadrature-phase (IQ) imbalance, which typically occur in the low-cost direct-conversion transmitter/receiver and cannot be avoided in AmBC [12]. It is important to understand how these HIs impact the performance of AmBC. To date, only two works considered HIs in AmBC. In [13], the authors proposed to jointly estimate the parameters of HIs, while in [14], the authors investigated the outage performance of the AmBC under HIs. However, the symbol detection under IQ imbalances has not been studied for AmBC, that is, the impacts of IQ imbalance on the symbol detection are still an open issue and worthy of investigation.

In this paper, we model and analyze the BER of the energy difference based detector in the presence of IQ imbalances. We derive a closed-form expression of the achievable BER as a function of the detection threshold and IQ imbalance parameters. The near-optimal detection threshold that results in a near-minimum BER is also derived. Considering that a priori knowledge of the CSI, the IQ imbalance parameters, the noise power and the transmit power of the ambient source is required by the AmBC receiver to calculate the near-optimal detection threshold, which hinders its application in practice, we devise a practical way to estimate the near-optimal detection threshold by exploiting the received signal samples at the AmBC receiver. Please note that the analysis of this paper can be extended into other energy-based detectors as we have derived the distribution of average power of the received signal corresponding to one backscatter bit that is a key point for analyzing the performance of energy-based detectors. Finally, computer simulations are performed to reveal the accuracy of our derived results and confirm the following findings. First, IQ imbalance degrades the BER of the studied symbol detector. Particularly, the phase imbalance degrades the BER of the studied detector more significantly than the amplitude imbalance. Second, the IQ imbalance has an impact

Yinghui Ye, Jiajia Zhao and Guangyue are with the Shaanxi Key Laboratory of Information Communication Network and Security, Xi'an University of Posts & Telecommunications, China.

Xiaoli Chu is with the Department of Electronic and Electrical Engineering, The University of Sheffield, U.K. (e-mail: x.chu@sheffield.ac.uk)

Sumei Sun is with the Institute of Infocomm Research, Agency for Science, Technology and Research, Singapore. (e-mail: sunsm@i2r.a-star.edu.sg)

on the near-optimal threshold. For example, when the relative phase deviation increases and the relative amplitude decreases simultaneously, the near-optimal threshold decreases.

The main notations used in this paper are listed below. $\mathbb{E}[x]$, $\mathrm{var}[x]$, and $|x|$ denote the expectation, the variance, and the absolute value of x, respectively. $Q(x) = \frac{1}{\sqrt{2\pi}}\int_x^{\infty}\exp\left(-\frac{t^2}{2}\right)dt$ is the Q function. $\mathbb{CN}(a,b)$ denotes the Gaussian distribution with mean a and variance b.

II. Signal Model

We consider an AmBC network with one ambient source, one AmBC transmitter, and an AmBC receiver, where the AmBC transmitter adopts differential encoding. We assume that all channels follow independent frequency flat block fading, i.e., all the channel fading coefficients keep constant in each transmission block, but may vary across adjacent blocks.

A. Signal Model under Perfect IQ Balance

Due to the modulation rate difference between the AmBC transmitter and the ambient source, we assume that one AmBC information bit is modulated into N consecutive ambient source information bits. The N consecutive samples at the AmBC receiver under perfect IQ balance are given by [6]

$$y^{\mathrm{ideal}}(n) = \mu(k)\, s(n) + w(n), n = 1, 2, \cdots, N, \tag{1}$$

where the superscript 'ideal' denotes the ideal scenario with perfect IQ balance, $\mu(k) = h + fgB(k)$, in which h, f and g are the complex channel coefficient of the ambient source to the AmBC receiver, the ambient source to the AmBC transmitter, and the AmBC transmitter to the AmBC receiver, respectively, $B(k) = A(k) \otimes B(k-1)$ $(k = 1, 2, \cdots, K)$ is the k-th output bit of the differential encoder at the AmBC transmitter, $A(k)$ denotes the k-th information bit input to the differential encoder, $\otimes$ denotes modulo 2 addition, $s(n) \sim \mathbb{CN}(0, P_s)$ and $w(n) \sim \mathbb{CN}(0, \sigma_w^2)$ are the n-th ambient source information bit and the additive white Gaussian noise, respectively, and P_s is the ambient source's transmit power.

By exploiting the feature of the differential encoder, an energy difference based detector [6] is adopted to detect $A(k)$ from $y^{\mathrm{ideal}}(n)$, i.e.,

$$\begin{cases} \hat{A}(k) = 1, \text{ if } \Phi_k^{\mathrm{ideal}} \triangleq \left|\Gamma_k^{\mathrm{ideal}} - \Gamma_{k-1}^{\mathrm{ideal}}\right| \geq \gamma_{\mathrm{th}}^{\mathrm{ideal}} \\ \hat{A}(k) = 0, \text{ if } \Phi_k^{\mathrm{ideal}} \triangleq \left|\Gamma_k^{\mathrm{ideal}} - \Gamma_{k-1}^{\mathrm{ideal}}\right| < \gamma_{\mathrm{th}}^{\mathrm{ideal}} \end{cases}, \tag{2}$$

where $\Gamma_k^{\mathrm{ideal}} = \frac{1}{N}\sum_{n=(k-1)N+1}^{kN}\left|y^{\mathrm{ideal}}(n)\right|^2$, which approximately follows a Gaussian distribution [6], is the average power of the N consecutive samples corresponding to $B(k)$, $\gamma_{\mathrm{th}}^{\mathrm{ideal}}$ is the detection threshold under perfect IQ balance, and $\hat{A}(k)$ is the estimated value of $A(k)$.

The corresponding BER and the near-optimal detection threshold can be, respectively, written as [6]

$$\begin{aligned} \mathbb{P}_{\mathrm{BER}}^{\mathrm{ideal}} &= \Pr\left(\hat{A}(k) = 0 \,|A(k) = 1\right)\Pr\left(A(k) = 1\right) \\ &+ \Pr\left(\hat{A}(k) = 1 \,|A(k) = 0\right)\Pr\left(A(k) = 0\right) \\ &= \frac{1}{2}Q\left(\frac{\gamma_{\mathrm{th}}^{\mathrm{ideal}}}{\sqrt{2\varsigma_0^2}}\right) - \frac{1}{2}Q\left(\frac{\gamma_{\mathrm{th}}^{\mathrm{ideal}} + \delta^{\mathrm{ideal}}}{\sqrt{\varsigma_0^2 + \varsigma_1^2}}\right) \\ &+ \frac{1}{2}Q\left(\frac{\gamma_{\mathrm{th}}^{\mathrm{ideal}}}{\sqrt{2\varsigma_1^2}}\right) + \frac{1}{2}Q\left(\frac{-\gamma_{\mathrm{th}}^{\mathrm{ideal}} + \delta^{\mathrm{ideal}}}{\sqrt{\varsigma_0^2 + \varsigma_1^2}}\right), \end{aligned} \tag{3}$$

$$\gamma_{\mathrm{th,nopt}}^{\mathrm{ideal}} = \frac{\left|\delta^{\mathrm{ideal}}\right|}{2} + \frac{\varsigma_0^2 + \varsigma_1^2}{\left|\delta^{\mathrm{ideal}}\right|}\ln\left(1 + \sqrt{1 - e^{-\frac{\left(\delta^{\mathrm{ideal}}\right)^2}{\varsigma_0^2 + \varsigma_1^2}}}\right), \tag{4}$$

where $\delta^{\mathrm{ideal}} = \mathbb{E}\left[\Gamma_k^{\mathrm{ideal}}|B(k) = 1\right] - \mathbb{E}\left[\Gamma_k^{\mathrm{ideal}}|B(k) = 0\right]$, $\mathbb{E}\left[\Gamma_k^{\mathrm{ideal}}|B(k) = 0\right] = |h|^2 P_s + \sigma_w^2$, $\mathbb{E}\left[\Gamma_k^{\mathrm{ideal}}|B(k) = 1\right] = |h + fg|^2 P_s + \sigma_w^2$, $\varsigma_0^2 = \mathrm{var}\left[\Gamma_k^{\mathrm{ideal}}|B(k) = 0\right] = \frac{2}{N}|h|^2 P_s \sigma_w^2$, and $\varsigma_1^2 = \mathrm{var}\left[\Gamma_k^{\mathrm{ideal}}|B(k) = 1\right] = \frac{2}{N}|h + fg|^2 P_s \sigma_w^2$.

Since the CSI, P_s, and σ_w^2 are not readily known by the AmBC receiver, $\gamma_{\mathrm{th,nopt}}^{\mathrm{ideal}}$ can not be obtained in practical AmBC. For the energy difference based detector in [6], by ignoring the second term in (4), $\gamma_{\mathrm{th}}^{\mathrm{ideal}}$ was estimated as $\frac{\mathbb{E}\left[\left|\Phi_k^{\mathrm{ideal}}\right|\right]}{2}$, where $\mathbb{E}\left[\left|\Phi_k^{\mathrm{ideal}}\right|\right] = \frac{1}{K}\sum_{k=1}^{K}\left|\Phi_k^{\mathrm{ideal}}\right|$.

B. Signal Model and Symbol Detection under IQ Imbalance

Under IQ imbalance, the signal samples at the AmBC receiver can be written as [12]

$$\begin{aligned} y^{\mathrm{iq}}(n) &= \kappa_1 y^{\mathrm{ideal}}(n) + \kappa_2\left(y^{\mathrm{ideal}}(n)\right)^* = \kappa_1\mu(k)\, s(n) \\ &+ \kappa_2\mu^*(k)\, s^*(n) + \kappa_1 w(n) + \kappa_2 w^*(n), \end{aligned} \tag{5}$$

where $\kappa_1 = \frac{1+\rho e^{-j\phi}}{2}$, $\kappa_2 = \frac{1-\rho e^{j\phi}}{2}$, the symbol '$*$' denotes the complex conjugate, ϕ and ρ give the relative phase deviation from the quadrature (90 degree) phase shift and the relative amplitude imbalance between the I and Q branches. By comparing (5) with (1), it can be seen that $y^{\mathrm{iq}}(n) = y^{\mathrm{ideal}}(n)$ for $\phi = 0$ and $\rho = 1$, i.e., the perfect IQ balance is a special case of IQ imbalance.

Under IQ imbalance, the energy difference based detector to detect $A(k)$ from $y^{\mathrm{iq}}(n)$ can be written as

$$\begin{cases} \hat{A}(k) = 1, \text{ if } \Phi_k^{\mathrm{iq}} \triangleq \left|\Gamma_k^{\mathrm{iq}} - \Gamma_{k-1}^{\mathrm{iq}}\right| \geq \gamma_{\mathrm{th}}^{\mathrm{iq}} \\ \hat{A}(k) = 0, \text{ if } \Phi_k^{\mathrm{iq}} \triangleq \left|\Gamma_k^{\mathrm{iq}} - \Gamma_{k-1}^{\mathrm{iq}}\right| < \gamma_{\mathrm{th}}^{\mathrm{iq}} \end{cases}, \tag{6}$$

where $\gamma_{\mathrm{th}}^{\mathrm{iq}}$ is the detection threshold under IQ imbalance, and $\Gamma_k^{\mathrm{iq}} = \frac{1}{N}\sum_{n=(k-1)N+1}^{kN}\left|y^{\mathrm{iq}}(n)\right|^2$ $(k = 1, 2, \cdots, K)$. According to the central limit theorem (CLT), Γ_k^{iq} approximately follows a Gaussian distribution, the mean and variance of which will be presented in the next section. Please note that the IQ imbalance has impacts on the coherent detector[1], e.g., [15], and this will be studied in our future work.

III. BER and Detection Threshold under IQ Imbalance

One can see from (3) and (4) that the BER and the near-optimal detection threshold under perfect IQ balance are determined by the mean and variance of $\Gamma_k^{\mathrm{ideal}}$. Similarly, if the mean and variance of Γ_k^{iq} are derived, then the BER and

[1]As shown in (5), the signal samples are affected by the IQ imbalance parameters, i.e., ϕ and ρ. This indicates that ϕ and ρ will affect the probability density function (PDF) of signal samples and the coherent detector that is related with the PDF of signal samples.

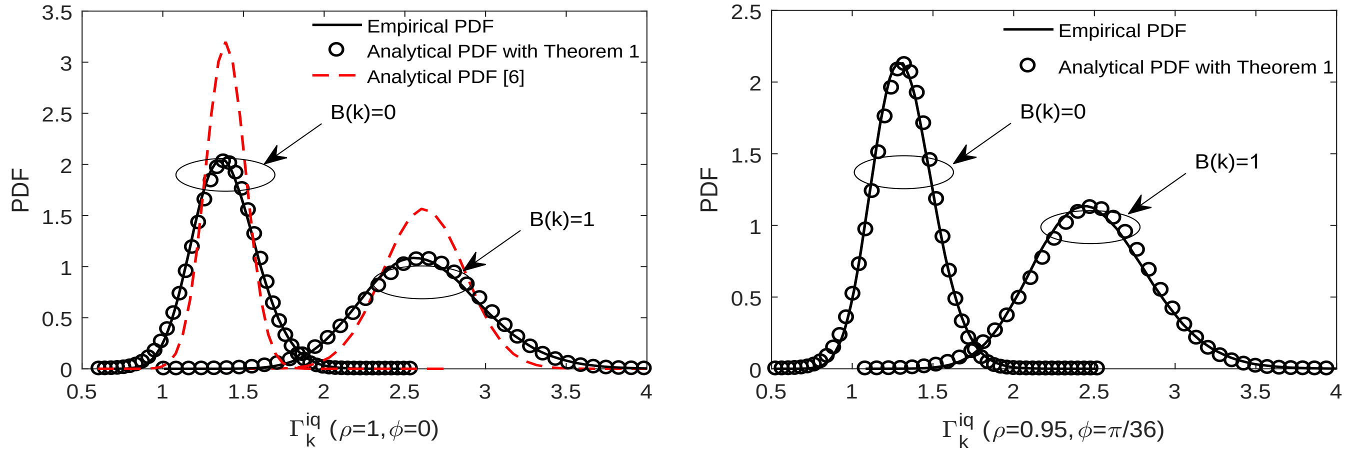

(a) (b)

Fig. 1. Empirical and analytical PDFs for $\Gamma_k^{\rm iq}$ with $N=50$, $\frac{P_s}{\sigma_w^2}=1$, $h=-0.1603-0.6026i$, and $h+fg=1.2272+0.3346i$: (a) perfect IQ balance; (b) IQ imbalance with $\rho=0.95$ and $\phi=\frac{\pi}{36}$.

near-optimal detection threshold under IQ imbalance can be obtained. Towards this end, Theorem 1 is provided.

Theorem 1. For given ϕ and ρ, the mean and variance of $\Gamma_k^{\rm iq}$ are, respectively, calculated as,

$$\begin{cases} \mathbb{E}\left[\Gamma_k^{\rm iq}\middle| B(k)=0\right] = \kappa\left(|h|^2 P_s+\sigma_w^2\right) \\ \mathbb{E}\left[\Gamma_k^{\rm iq}\middle| B(k)=1\right] = \kappa\left(|h+fg|^2 P_s+\sigma_w^2\right) \end{cases} \tag{7}$$

$$\begin{cases} \mathrm{var}\left[\Gamma_k^{\rm iq}\middle| B(k)=0\right] \simeq \frac{a\left(P_s|h|^2+\sigma_w^2\right)^2}{2N} \\ \mathrm{var}\left[\Gamma_k^{\rm iq}\middle| B(k)=1\right] \simeq \frac{a\left(P_s|h+fg|^2+\sigma_w^2\right)^2}{2N} \end{cases} \tag{8}$$

where $\kappa=\frac{1+\rho^2}{2}$, $a=\rho^4+1+2\rho^2\sin^2\phi$.

Proof. Please refer to Appendix A. ■

In Fig. 1 (a), for the case of perfect IQ balance (i.e., $\phi=0$ and $\rho=1$), we compare the empirical PDF of $\Gamma_k^{\rm ideal}$ with the approximated Gaussian PFD of $\Gamma_k^{\rm ideal}$ (with mean and variance given in (3) and (4)) provided by [6] and the approximated Gaussian PDF of $\Gamma_k^{\rm iq}$ (which equals $\Gamma_k^{\rm ideal}$ for $\phi=0$ and $\rho=1$) given in Theorem 1. We can see that for $\phi=0$ and $\rho=1$, i.e., the case of perfect IQ balance, Theorem 1 provides a much more accurate PDF of $\Gamma_k^{\rm ideal}$ than that given in [6]. This is because in [6], $\Gamma_k^{\rm ideal}$ was decomposed into two terms (see (10)-(13) in [6]) and one of them (i.e., (10) or (11) in [6]) was treated as a constant in approximating its variance, while in our work, we have not made any approximation in deriving its variance. Hence, our derived variance of $\Gamma_k^{\rm ideal}$ is more accurate than that of [6]. Besides, Fig. 1(b) shows that the analytical PDF of $\Gamma_k^{\rm iq}$ given by Theorem 1 matches closely the empirical PDF of $\Gamma_k^{\rm iq}$ under IQ imbalances.

Lemma 1. Using (7) and (8) to replace the conditional means and variances of $\Gamma_k^{\rm ideal}$ in (3) and (4), we obtain the expressions of the BER and the near-optimal detection threshold under IQ imbalances as follows,

$$\begin{aligned}\mathbb{P}_{\rm BER}^{\rm iq} = {} & \frac{1}{2}Q\left(\frac{\gamma_{\rm th}^{\rm iq}}{\sqrt{2\Delta_0^2}}\right)+\frac{1}{2}Q\left(\frac{\gamma_{\rm th}^{\rm iq}}{\sqrt{2\Delta_1^2}}\right) \\ & -\frac{1}{2}Q\left(\frac{\gamma_{\rm th}^{\rm iq}+\delta^{\rm iq}}{\sqrt{\Delta_0^2+\Delta_1^2}}\right)+\frac{1}{2}Q\left(\frac{-\gamma_{\rm th}^{\rm iq}+\delta^{\rm iq}}{\sqrt{\Delta_0^2+\Delta_1^2}}\right),\end{aligned} \tag{9}$$

$$\gamma_{\rm th,nopt}^{\rm iq} = \frac{\left|\delta^{\rm iq}\right|}{2}+\frac{\Delta_+^2}{\left|\delta^{\rm iq}\right|}\ln\left(1+\sqrt{1-e^{-\frac{\left(\delta^{\rm iq}\right)^2}{\Delta_+^2}}}\right), \tag{10}$$

where $\delta^{\rm iq} = \kappa P_s\left(|h+fg|^2-|h|^2\right)$, $\Delta_0^2 = \mathrm{var}\left[\Gamma_k^{\rm iq}\middle| B(k)=0\right]$, $\Delta_1^2 = \mathrm{var}\left[\Gamma_k^{\rm iq}\middle| B(k)=1\right]$, and $\Delta_+^2=\Delta_0^2+\Delta_1^2$.

One observation from (10) is that $\left|\delta^{\rm iq}\right|$ and Δ_+^2 are required to calculate the near-optimal detection threshold $\gamma_{\rm th,nopt}^{\rm iq}$. However, the exact values of $\left|\delta^{\rm iq}\right|$ and Δ_+^2 depend on the CSI, the IQ imbalance parameters ϕ and ρ, the noise power and the transmit power of the ambient source, which are unknown by the AmBC receiver. To address this problem, we devise a simple but practical way to estimate $\left|\delta^{\rm iq}\right|$ and Δ_+^2 as follows.

Lemma 2. Based on (B.2) of Appendix B, we have $\left|\delta^{\rm iq}\right| = \sqrt{2\left(\mathrm{var}\left[\Phi_k^{\rm iq}\right]-\Delta_+^2\right)}$, where Δ_+^2 can be obtained by solving the following equation for Δ_+, i.e.,

$$\begin{aligned}\mathbb{E}\left[\left|\Phi_k^{\rm iq}\right|\right] \approx {} & \sqrt{\frac{3}{8\pi}}\Delta_+ + \frac{\Delta_+}{\sqrt{2\pi}}\exp\left(-\frac{\mathrm{var}\left[\Phi_k^{\rm iq}\right]-\Delta_+^2}{\Delta_+^2}\right) \\ & +\sqrt{\frac{\mathrm{var}\left[\Phi_k^{\rm iq}\right]-\Delta_+^2}{\pi}}\int_0^{\frac{\sqrt{2\left(\mathrm{var}\left[\Phi_k^{\rm iq}\right]-\Delta_+^2\right)}}{\Delta_+}}\exp\left(-\frac{t^2}{2}\right)dt\end{aligned} \tag{11}$$

where $\Delta_+ < \sqrt{\mathrm{var}\left[\Phi_k^{\rm iq}\right]}$, and $\mathrm{var}\left[\Phi_k^{\rm iq}\right]=\frac{1}{K-1}\sum_{k=1}^{K}\left(\Phi_k^{\rm iq}\right)^2$ and $\mathbb{E}\left[\left|\Phi_k^{\rm iq}\right|\right]=\frac{1}{K}\sum_{k=1}^{K}\left|\Phi_k^{\rm iq}\right|$ hold for a sufficiently large K.

TABLE I

IQ imbalance parameter	Our theoretical $\gamma_{\mathrm{th,nopt}}^{\mathrm{iq}}$	Our estimated $\gamma_{\mathrm{th,nopt}}^{\mathrm{iq}}$	Theoretical $\gamma_{\mathrm{th,nopt}}^{\mathrm{ideal}}$ in [6]	Estimated $\gamma_{\mathrm{th,nopt}}^{\mathrm{ideal}}$ in [6]
$\rho = 1$, $\phi = 0$	20.4682	19.5989	19.4799	11.0101
$\rho = 0.95$, $\phi = \pi/36$	19.4804	18.6525	Not available	Not available
$\rho = 0.9$, $\phi = \pi/18$	18.5619	17.7560	Not available	Not available

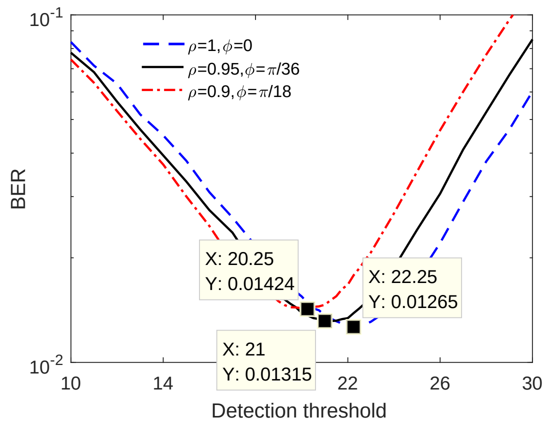

Fig. 2. BER versus Detection threshold.

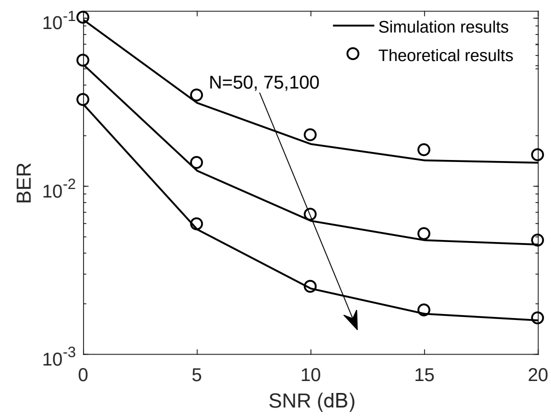

Fig. 3. BER versus SNR.

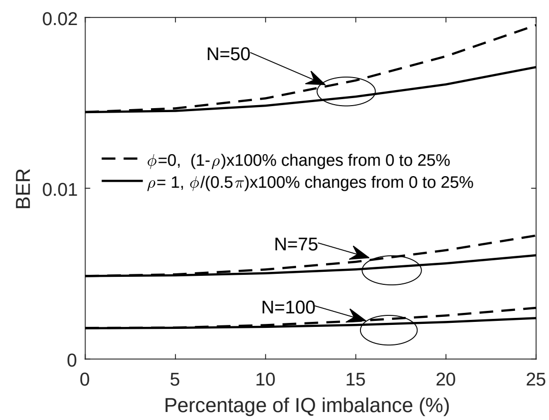

Fig. 4. BER versus $(1-\rho)\times 100\%$ or $\frac{\phi}{0.5\pi}\times 100\%$.

Proof. Please refer to Appendix B. ∎

Moving the third term on the right-hand side of (11) to the left-hand side, we have

$$\vartheta_1\left(\Delta_+\right) = \vartheta_2\left(\Delta_+\right), \tag{12}$$

where

$$\vartheta_1(\Delta_+) = \sqrt{\frac{3}{8\pi}}\Delta_+ + \frac{\Delta_+}{\sqrt{2\pi}}\exp\left(-\frac{\operatorname{var}\left[\Phi_k^{\mathrm{iq}}\right]-\Delta_+^2}{\Delta_+^2}\right), \tag{13}$$

$$\vartheta_2\left(\Delta_+\right) = \mathbb{E}\left[\left|\Phi_k^{\mathrm{iq}}\right|\right] - \sqrt{\frac{\operatorname{var}\left[\Phi_k^{\mathrm{iq}}\right]-\Delta_+^2}{\pi}} \times \int_0^{\frac{\sqrt{2\left(\operatorname{var}\left[\Phi_k^{\mathrm{iq}}\right]-\Delta_+^2\right)}}{\Delta_+}} \exp\left(-\frac{t^2}{2}\right)dt. \tag{14}$$

We note that $\vartheta_1(\Delta_+)$ and $\vartheta_2\left(\Delta_+\right)$ are increasing functions of Δ_+ for $\Delta_+ > 0$. Since $\frac{\partial\vartheta_1(\Delta_+)}{\partial\Delta_+} \neq \frac{\partial\vartheta_2(\Delta_+)}{\partial\Delta_+}$ and $0 < \Delta_+ < \sqrt{\operatorname{var}\left[\Phi_k^{\mathrm{iq}}\right]}$, there exists a solution satisfying $\vartheta_1\left(\Delta_+\right) = \vartheta_2\left(\Delta_+\right)$ in the open interval $\left(0, \sqrt{\operatorname{var}\left[\Phi_k^{\mathrm{iq}}\right]}\right)$. This value of Δ_+ can be found by one-dimension search methods. Once the value of Δ_+ satisfying (11) is obtained, $\left|\delta^{\mathrm{iq}}\right|$ can be calculated following Lemma 2. Substituting the values of Δ_+ and $\left|\delta^{\mathrm{iq}}\right|$ into (10), the near-optimal detection threshold under IQ imbalance can be obtained.

IV. Simulation Result

The basic parameters are the same as those of Fig. 1. Unless otherwise stated, the signal-to-noise ratio (SNR), $10\log\frac{P_s}{\sigma_w^2}$, is set as 15 dB. In Fig. 2, we study the relationships between BER and detection threshold under different IQ imbalance parameters, respectively. It can be seen that there exists an optimal detection threshold minimizing BER and that the optimal detection threshold decreases with the IQ imbalance. This is because the IQ imbalance decreases the mean of Δ_+^2 and $\frac{\gamma_{\mathrm{th,nopt}}^{\mathrm{iq}}}{2}$ is the dominant one to calculate $\gamma_{\mathrm{th,nopt}}^{\mathrm{iq}}$. Table I lists the theoretical and estimated near-optimal detection thresholds. Our theoretical and estimated detection thresholds are calculated by (10) using the exact and estimated $\left|\delta^{\mathrm{iq}}\right|$ and Δ_+^2, respectively. The theoretical and estimated detection thresholds provided in [6] are calculated by (4) and $\frac{\mathbb{E}\left[\left|\Phi_k^{\mathrm{ideal}}\right|\right]}{2}$, respectively. By comparisons between the optimal detection threshold shown in Fig. 2 and the near-optimal detection threshold listed in Table I, one can see that our theoretical and estimated thresholds are closer to the optimal one than those of [6] particularly for the estimated threshold. The main reason is that the second term of (4) is ignored in [6] while it is considered in our estimated one. One can also see from Table I that our theoretical and estimated thresholds decrease when ϕ increases and ρ decreases simultaneously.

Fig. 3 plots the BER versus SNR under the perfect IQ balance. The threshold is calculated by (10). It can be seen that our derived BER matches simulation results well and the accuracy of (10) increases with N. This validates the correctness of our derived BER. It can also be seen that an error floor exists. This is because the AmBC receiver suffers from the direct link interference caused by the ambient source, the same as the IQ balance case in [6].

In Fig. 4, we evaluate the impact of IQ imbalance on the BER of the energy difference based detector. The percentages of the amplitude and phase imbalances are calculated as $(1-\rho)\times 100\%$ and $\frac{\phi}{\pi/2}\times 100\%$, respectively. One can see that the BER increases with the percentage IQ imbalance, which indicates that IQ imbalance degrades the performance. One can also see that the performance degradation of the phase imbalance is higher than that of the amplitude imbalance. This indicates that the energy difference based detector is more sensitive to the phase imbalance over the amplitude imbalance.

Finally, we study the impacts of K on the estimated threshold in Fig. 5. One can see that for all the considered values of K, our estimated threshold is closer to the theoretical one than the estimated threshold provided in [6]. One can also see that our estimated threshold approaches the theoretical threshold when K increases. This is because a larger K results in a more accurate approximation on $\mathrm{var}\left[\Phi_k^{\mathrm{iq}}\right]$ and $\mathbb{E}\left[\left|\Phi_k^{\mathrm{iq}}\right|\right]$.

V. Conclusion

In this paper, we have derived the BER and the near-optimal detection threshold of the energy difference based detector for differentially encoded AmBC in the presence of IQ imbalances. We have proposed a method to estimate the near-optimal detection threshold so that a blind symbol detection can be achieved. Our simulation results have validated the accuracy of the analytical results and shown that the energy difference based detector is more robust to the amplitude imbalance than to the phase imbalance in terms of BER.

Appendix A

Based on (5), Γ_k^{iq} can be calculated as

$$\begin{aligned}\Gamma_k^{\mathrm{iq}} &= \frac{1}{N}\sum_{n=(k-1)N+1}^{kN}\left|y^{\mathrm{iq}}(n)\right|^2\\ &= \frac{1}{N}\sum_{n=(k-1)N+1}^{kN}\left(a_1\mathrm{Re}^2\left[y_d^{\mathrm{ideal}}(n)\right]+a_2\mathrm{Im}^2\left[y_d^{\mathrm{ideal}}(n)\right]\right)\\ &+\frac{1}{N}\sum_{n=(k-1)N+1}^{kN}2a_3\mathrm{Re}\left[y_d^{\mathrm{ideal}}(n)\right]\mathrm{Im}\left[y_d^{\mathrm{ideal}}(n)\right],\end{aligned} \tag{A.1}$$

where $a_1 = 1+\rho^2\sin^2\varphi$, $a_2=\rho^2\cos^2\varphi$, and $a_3 = -\rho^2\cos\varphi\sin\varphi$.

Then, the mean of Γ_k^{iq} is given by

$$\begin{aligned}\mathbb{E}\left[\Gamma_k^{\mathrm{iq}}\right] &= \frac{a_1}{N}\sum_{n=(k-1)N+1}^{kN}\mathbb{E}\left[\mathrm{Re}^2\left[y_d^{\mathrm{ideal}}(n)\right]\right]\\ &+\frac{2a_3}{N}\sum_{n=(k-1)N+1}^{kN}\mathbb{E}\left[\mathrm{Re}\left[y_d^{\mathrm{ideal}}(n)\right]\right]\mathbb{E}\left[\mathrm{Im}\left[y_d^{\mathrm{ideal}}(n)\right]\right]\\ &+\frac{a_2}{N}\sum_{n=(k-1)N+1}^{kN}\mathbb{E}\left[\mathrm{Im}^2\left[y_d^{\mathrm{ideal}}(n)\right]\right]\end{aligned}$$

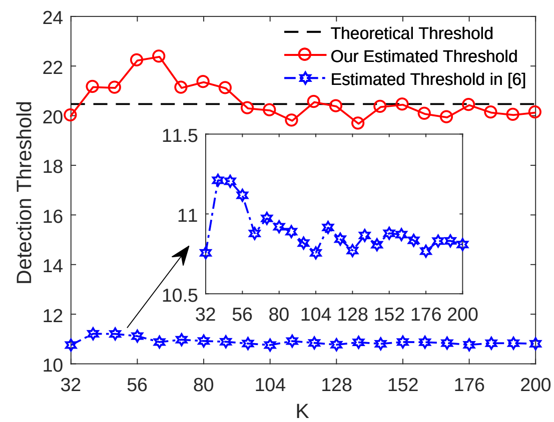

Fig. 5. Detection threshold versus K.

$$= \begin{cases}\kappa\left(|h|^2P_s+\sigma_w^2\right), & B(k)=0\\ \kappa\left(|h+fg|^2P_s+\sigma_w^2\right), & B(k)=1\end{cases}, \tag{A.2}$$

where $\kappa = \frac{1+\rho^2}{2}$. Due to the symmetry in IQ branches, $\mathbb{E}\left[\mathrm{Re}^2\left[y_d^{\mathrm{ideal}}(n)\right]\right] = \mathbb{E}\left[\mathrm{Im}^2\left[y_d^{\mathrm{ideal}}(n)\right]\right] = \frac{1}{2}\mathbb{E}\left[\left|y_d^{\mathrm{ideal}}(n)\right|^2\right]$ holds. Combining with $\mathbb{E}\left[y_d^{\mathrm{ideal}}(n)\right]=0$, and $\mathbb{E}\left[\Gamma_k^{\mathrm{ideal}}\right]=\mathbb{E}\left[\left|y_d^{\mathrm{ideal}}(n)\right|^2\right]$, the last equality is derived.

The variance of T_k^{iq} is written as (A.3), as shown at the top of the next page, whose value of each term in (A.3) is derived as follows. Applying CLT and the symmetry in IQ branches, it is not hard to derive that both $\sum_{n=(k-1)N+1}^{kN}\mathrm{Re}^2\left[y_d^{\mathrm{ideal}}(n)\right]$ and $\sum_{n=(k-1)N+1}^{kN}\mathrm{Im}^2\left[y_d^{\mathrm{ideal}}(n)\right]$ follow the Gaussian distribution with a mean $\frac{N\mathbb{E}[\Gamma_k]}{2}$ and a variance $\frac{N\mathbb{E}^2[\Gamma_k]}{2}$ when N is sufficient large. Similar as above, $\sum_{n=(k-1)N+1}^{kN}\mathrm{Re}\left[y_d^{\mathrm{ideal}}(n)\right]\mathrm{Im}\left[y_d^{\mathrm{ideal}}(n)\right]$ obeys the Gaussian distribution with a mean zero and a variance $\frac{N\mathbb{E}^2[\Gamma_k]}{4}$. Until now, it is easy to determine the values for the first three terms. Then we put our attention on calculating the values of the last two terms. Through some convenient mathematical calculations, we obtain (A.4), as shown at the top of the next page, where the last equality holds from $\mathbb{E}\left[\mathrm{Re}^3\left[y_d^{\mathrm{ideal}}(n)\right]\right] = \mathbb{E}\left[\mathrm{Re}\left[y_d^{\mathrm{ideal}}(n)\right]\right]=0$. Similarly, it can be concluded that the last term of (A.3) equals zero. Based on the above analyses, (A.3) can be approximated as $\frac{\left(\rho^4+1+2\rho^2\sin^2\phi\right)\mathbb{E}^2[\Gamma_k]}{2N}$.

Appendix B

Applying CLT, it is easy to know Γ_k^{iq} is approximated as a Gaussian distribution. Combining this with Theorem 1, the probability density function (PDF) of Φ_k^{iq} is approximated as

$$\Phi_k^{\mathrm{iq}} \sim \begin{cases}\mathcal{CN}\left(0,2\Delta_0^2\right), & \text{if } B(k)=0, B(k-1)=0\\ \mathcal{CN}\left(0,2\Delta_1^2\right), & \text{if } B(k)=1, B(k-1)=1\\ \mathcal{CN}\left(\delta^{\mathrm{iq}},\Delta_+^2\right), & \text{if } B(k)=1, B(k-1)=0\\ \mathcal{CN}\left(-\delta^{\mathrm{iq}},\Delta_+^2\right), & \text{if } B(k)=0, B(k-1)=1\end{cases} \tag{B.1}$$

Based on (B.1), the mean and the mean square value of Φ_k^{iq} equal $\delta^{\mathrm{iq}}\left(p_{b,10}-p_{b,01}\right)$ and $2\Delta_0^2p_{b,00}+2\Delta_1^2p_{b,11}+\left(\left(\delta^{\mathrm{iq}}\right)^2+\Delta_+^2\right)\left(p_{b,10}+p_{b,01}\right)$, respectively, where $p_{b,mn} =$

$$\operatorname{var}\left[\Gamma_k^{\mathrm{iq}}\right]=\frac{a_1^2}{N^2}\operatorname{var}\left[\sum_{n=(k-1)N+1}^{kN}\operatorname{Re}^2\left[y_d^{\mathrm{ideal}}(n)\right]\right]+\frac{4a_3^2}{N^2}\operatorname{var}\left[\sum_{n=(k-1)N+1}^{kN}\operatorname{Re}\left[y_d^{\mathrm{ideal}}(n)\right]\operatorname{Im}\left[y_d^{\mathrm{ideal}}(n)\right]\right]+\frac{a_2^2}{N^2}$$
$$\times\operatorname{var}\left[\sum_{n=(k-1)N+1}^{kN}\operatorname{Im}^2\left[y_d^{\mathrm{ideal}}(n)\right]\right]+\frac{4a_1a_3}{N^2}\operatorname{cov}\left(\sum_{n=(k-1)N+1}^{kN}\operatorname{Re}^2\left[y_d^{\mathrm{ideal}}(n)\right],\sum_{n=(k-1)N+1}^{kN}\operatorname{Re}\left[y_d^{\mathrm{ideal}}(n)\right]\operatorname{Im}\left[y_d^{\mathrm{ideal}}(n)\right]\right)$$
$$+\frac{4a_2a_3}{N^2}\operatorname{cov}\left(\sum_{n=(k-1)N+1}^{kN}\operatorname{Im}^2\left[y_d^{\mathrm{ideal}}(n)\right],\sum_{n=(k-1)N+1}^{kN}\operatorname{Re}\left[y_d^{\mathrm{ideal}}(n)\right]\operatorname{Im}\left[y_d^{\mathrm{ideal}}(n)\right]\right). \tag{A.3}$$

$$\operatorname{cov}\left(\sum_{n=(k-1)N+1}^{kN}\operatorname{Re}^2\left[y_d^{\mathrm{ideal}}(n)\right],\sum_{n=(k-1)N+1}^{kN}\operatorname{Re}\left[y_d^{\mathrm{ideal}}(n)\right]\operatorname{Im}\left[y_d^{\mathrm{ideal}}(n)\right]\right)$$
$$=\sum_{n=(k-1)N+1}^{kN}\mathbb{E}\left[\operatorname{Im}\left[y_d^{\mathrm{ideal}}(n)\right]\right]\left(\mathbb{E}\left[\operatorname{Re}^3\left[y_d^{\mathrm{ideal}}(n)\right]\right]-\mathbb{E}\left[\operatorname{Re}^2\left[y_d^{\mathrm{ideal}}(n)\right]\right]\mathbb{E}\left[\operatorname{Re}\left[y_d^{\mathrm{ideal}}(n)\right]\right]\right)=0, \tag{A.4}$$

$\Pr\left(B(k)=m,B(k-1)=n\right)$, $m,n\in\{0,1\}$. Due to the equiprobable backscattered messages, $A(k)=0$ and $A(k)=1$, and the adopted differential encoding scheme at the AmBC transmitter, $p_{b,00}=p_{b,11}=p_{b,10}=p_{b,01}=\frac{1}{4}$. Thus, we have

$$\operatorname{var}\left[\Phi_k^{\mathrm{iq}}\right]=\mathbb{E}\left[\left(\Phi_k^{\mathrm{iq}}\right)^2\right]-\mathbb{E}^2\left[\Phi_k^{\mathrm{iq}}\right]=\frac{\left(\delta^{\mathrm{iq}}\right)^2}{2}+\Delta_+^2, \tag{B.2}$$

where the second equality holds from $\mathbb{E}\left[\Phi_k^{\mathrm{iq}}\right]=0$. Similar as above, it is not hard to derive $\mathbb{E}\left[\Phi_k^{\mathrm{iq}}\right]=0$. Since Φ_k^{iq} follows the Gaussian distribution, $\left|\Phi_k^{\mathrm{iq}}\right|$ obeys the folded normal distribution and its mean can be calculated as [16]

$$\begin{aligned}\mathbb{E}\left[\left|\Phi_k^{\mathrm{iq}}\right|\right]&=\frac{(\Delta_0+\Delta_1)}{2\sqrt{\pi}}+\frac{\Delta_+}{\sqrt{2\pi}}\exp\left(-\frac{\left(\delta^{\mathrm{iq}}\right)^2}{2\Delta_+^2}\right)\\&\quad+\frac{1}{2}\delta^{\mathrm{iq}}\left[Q\left(-\frac{\delta^{\mathrm{iq}}}{\Delta_+}\right)-Q\left(\frac{\delta^{\mathrm{iq}}}{\Delta_+}\right)\right]\\&\overset{(a)}{\approx}\sqrt{\frac{3}{8\pi}}\Delta_++\frac{\Delta_+}{\sqrt{2\pi}}\exp\left(-\frac{\left(\delta^{\mathrm{iq}}\right)^2}{2\Delta_+^2}\right)\\&\quad+\frac{\left|\delta^{\mathrm{iq}}\right|}{\sqrt{2\pi}}\int_0^{\frac{\left|\delta^{\mathrm{iq}}\right|}{\Delta_+}}\exp\left(-\frac{t^2}{2}\right)dt,\end{aligned} \tag{B.3}$$

where step (a) holds from $\left(\Delta_0+\Delta_1\right)^2=\Delta_+^2+2\Delta_0\Delta_1\approx\frac{3}{2}\Delta_+^2$, $\int_0^{\frac{\delta^{\mathrm{iq}}}{\Delta_+}}\exp\left(-\frac{t^2}{2}\right)dt=\int_{-\frac{\delta^{\mathrm{iq}}}{\Delta_+}}^0\exp\left(-\frac{t^2}{2}\right)dt$, and $\delta^{\mathrm{iq}}\int_0^{\frac{\delta^{\mathrm{iq}}}{\Delta_+}}\exp\left(-\frac{t^2}{2}\right)dt=\left|\delta^{\mathrm{iq}}\right|\int_0^{\frac{\left|\delta^{\mathrm{iq}}\right|}{\Delta_+}}\exp\left(-\frac{t^2}{2}\right)dt$.

References

[1] C. Xu, L. Yang, and P. Zhang, "Practical backscatter communication systems for battery-free internet of things: A tutorial and survey of recent research," *IEEE Signal Process. Mag.*, vol. 35, no. 5, pp. 16–27, 2018.

[2] Y. Ye, L. Shi, X. Chu, and G. Lu, "On the outage performance of ambient backscatter communications," *IEEE Internet Things J.*, vol. 7, no. 8, pp. 7265–7278, 2020.

[3] V. Liu, A. Parks, V. Talla, S. Gollakota, D. Wetherall, and J. R. Smith, "Ambient backscatter: Wireless communication out of thin air," *ACM SIGCOMM Comput. Commun. Rev.*, vol. 43, no. 4, pp. 39–50, 2013.

[4] K. Lu, G. Wang, F. Qu, and Z. Zhong, "Signal detection and ber analysis for RF-powered devices utilizing ambient backscatter," in *Proc. IEEE WCSP*, 2015, pp. 1–5.

[5] J. Qian, F. Gao, G. Wang, S. Jin, and H. Zhu, "Noncoherent detections for ambient backscatter system," *IEEE Trans. Wireless Commun.*, vol. 16, no. 3, pp. 1412–1422, 2017.

[6] G. Wang, F. Gao, R. Fan, and C. Tellambura, "Ambient backscatter communication systems: Detection and performance analysis," *IEEE Trans. Commun.*, vol. 64, no. 11, pp. 4836–4846, 2016.

[7] J. Qian, A. N. Parks, J. R. Smith, F. Gao, and S. Jin, "Iot communications with m-PSK modulated ambient backscatter: Algorithm, analysis, and implementation," *IEEE Internet Things J.*, vol. 6, no. 1, pp. 844–855, 2019.

[8] Q. Tao, C. Zhong, X. Chen, H. Lin, and Z. Zhang, "Maximum-eigenvalue detector for multiple antenna ambient backscatter communication systems," *IEEE Trans. Veh. Technol.*, vol. 68, no. 12, pp. 12 411–12 415, 2019.

[9] C. Chen, G. Wang, P. D. Diamantoulakis, R. He, G. K. Karagiannidis, and C. Tellambura, "Signal detection and optimal antenna selection for ambient backscatter communications with multi-antenna tags," *IEEE Trans. Commun.*, vol. 68, no. 1, pp. 466–479, 2020.

[10] G. Yang, Y.-C. Liang, R. Zhang, and Y. Pei, "Modulation in the air: Backscatter communication over ambient OFDM carrier," *IEEE Trans. Commun.*, vol. 66, no. 3, pp. 1219–1233, 2018.

[11] C. Liu, Z. Wei, D. W. K. Ng, J. Yuan, and Y.-C. Liang, "Deep transfer learning for signal detection in ambient backscatter communications," *IEEE Trans. Wireless Commun.*, vol. 20, no. 3, pp. 1624–1638, 2021.

[12] M. Valkama, M. Renfors, and V. Koivunen, "Advanced methods for I/Q imbalance compensation in communication receivers," *IEEE Trans. Signal Process.*, vol. 49, no. 10, pp. 2335–2344, 2001.

[13] S. Abdallah, A. I. Salameh, and M. Saad, "Joint channel, carrier frequency offset and I/Q imbalance estimation in ambient backscatter communication systems," *IEEE Commun. Lett.*, vol. 25, no. 7, pp. 2250–2254, 2021.

[14] X. Li, M. Zhao, M. Zeng, S. Mumtaz, V. G. Menon, Z. Ding, and O. A. Dobre, "Hardware impaired ambient backscatter NOMA systems: Reliability and security," *IEEE Trans. on Commun.*, vol. 69, no. 4, pp. 2723–2736, 2021.

[15] Z. Niu, W. Ma, W. Wang, and T. Jiang, "Spatial modulation-based ambient backscatter: Bringing energy self-sustainability to massive internet of everything in 6G," *China Commun.*, vol. 17, no. 12, pp. 52–65, 2020.

[16] F. C. Leone, L. S. Nelson, and R. Nottingham, "The folded normal distribution," *Technometrics*, vol. 3, no. 4, pp. 543–550, 1961.